Acta Crystallographica Section D
Biological Crystallography
ISSN 0907-4449

Co-expression, copurification, crystallization and preliminary X-ray analysis of a complex of ARL2-GTP and PDE δ

Louis Renault,†‡ Michael Hanzal-Bayer† and Roman C. Hillig*§

Max-Planck-Institut für Molekulare Physiologie, Abteilung Strukturelle Biologie, Otto-Hahn-Strasse 11, 44227 Dortmund, Germany

† These authors contributed equally.
‡ Present address: Laboratoire d'Enzymologie et Biochimie Structurales, CNRS, Avenue de la Terrasse, 91198 Gif-sur-Yvette, France.
§ Present address: Institut für Immungenetik, Universitätsklinikum Charité, Humboldt-Universität zu Berlin, Spandauer Damm 130, 14050 Berlin, Germany.

Correspondence e-mail: roman.hillig@mpi-dortmund.mpg.de

Received 10 May 2001
Accepted 8 June 2001

The small GTPase ARL2 (from *Mus musculus*) and an effector protein, the δ subunit of human cGMP phosphodiesterase (hPDE δ), were co-expressed and copurified from *Escherichia coli* as a stable complex. Co-expression significantly increased the otherwise low yield of PDE δ production in *E. coli*. The complex, which contains ARL2 in the activated GTP-bound form, was crystallized in two forms. The first belonged to the monoclinic space group $P2_1$, with unit-cell parameters a = 48.1, b = 45.7, c = 74.7 Å, β = 94.0° and one complex (39 kDa) in the asymmetric unit. Cryocooled crystals diffracted to 2.3 Å using synchrotron radiation. The microfocused X-ray beam at beamline ID13 (ESRF) allowed the use of very small crystals, which helped to overcome twinning and enabled the identification of a molecular-replacement solution. The second form recrystallized from the first one after several months. These crystals belonged to the orthorhombic space group $P2_12_12_1$, with unit-cell parameters a = 44.5, b = 65.4, c = 104.4 Å and one complex in the asymmetric unit. They diffracted to 1.8 Å using synchrotron radiation.

1. Introduction

The ADP-ribosylation factor (ARF) family is part of the Ras superfamily of small GTPases and is subdivided into the ARF group (Kahn & Gilman, 1984) and the group of ARF-like (ARL) proteins (Tamkun *et al.*, 1991). Ras-like GTPases act as molecular switches, cycling between an inactive GDP-bound and an activated GTP-bound state and are involved in the regulation of a wide variety of cellular processes. Both ARF and ARL proteins are expressed in several isoforms in many tissues. For ARF proteins, the individual isoforms are targeted to different cellular membrane compartments. While the physiological role of ARF proteins is the regulation of vesicle formation in intracellular traffic (Moss & Vaughan, 1998; Chavrier & Goud, 1999), the role of ARL proteins is not yet understood. The δ subunit of the human cGMP phosphodiesterase (hPDE δ) was identified as an interaction partner of RPGR (retinitis pigmentosa guanine regulator), a protein responsible for the human hereditary eye disease X-linked retinitis pigmentosa type III (Linari, Ueffing *et al.*, 1999). PDE δ then turned out to interact in a GTP-dependent manner with ARL3 (Linari, Hanzal-Bayer *et al.*, 1999) and ARL2 (M. Hanzal-Bayer, unpublished data), thus representing a putative effector protein for this group of small GTPases. PDE δ binds specifically to ARL3-GTP and stabilizes this nucleotide state, thereby increasing the otherwise low affinity of ARL3 for GTP (Linari, Hanzal-Bayer *et al.*, 1999). As a first step towards understanding ARL proteins on the molecular level, we recently determined the structure of ARL3-GDP (Hillig *et al.*, 2000). It revealed an overall high similarity to ARF1-GDP (Amor *et al.*, 1994; Greasley *et al.*, 1995), including an unusual position of the 'interswitch region' between switch 1 and switch 2. This region constitutes an ARF-specific third switch by which conformational changes of the G domain modulate membrane affinity in the ARF group (Antonny *et al.*, 1997; Goldberg, 1998; Béraud-Dufour *et al.*, 1999). We have initiated a structural analysis of the complex of ARL2-GTP and PDE δ. This complex will reveal the conformation of an ARL protein in its GTP-bound form which, by comparison with the closely related ARL3-GDP, will allow the precise assignment of the switch regions in this group of GTPases. Knowledge of the exact conformation of the GTPase is of particular interest in the ARF family because ARF isoforms are highly homologous and small differences at the sequence and structure level appear to determine targeting to their specific cellular compartments and interaction with their specific effectors and regulators (Menetrey *et al.*, 2000). Moreover, the structures of ARL2-GTP and PDE δ will provide the first structural insights into the interaction between

an effector of the ARF family and its GTPase. As the physiological function of PDE δ as an effector of ARL proteins is not yet clear, we expect the structure of the complex to shed light on the role of this interaction.

2. Methods and materials

The open reading frames of murine ARL2 (GenBank AF143680) and human PDE δ (GenBank AF045999) were inserted as a *Bam*HI/*Hin*dIII fragment into pGEX KG (GST-ARL2) and as a *Bam*HI/*Xho*I fragment into pET28a (His-PDEδ), respectively. Cells of the methionine auxotroph *E. coli* strain B834 (Novagen) were transformed with both plasmids simultaneously and each colony obtained was tested for co-expression of both proteins. Strain B834 was chosen to enable production of the selenomethionine-labelled proteins at a later stage (see below). The cells were used to inoculate a 5 l culture in Terrific Broth medium supplemented with 50 µg ml^{-1} ampicillin and 25 µg ml^{-1} kanamycin. Cells were grown at 310 K to an OD_{600} of 0.8, whereupon expression was induced with 0.6 m*M* IPTG. After 1 h at 310 K, incubation was prolonged at 291 K overnight. Cells were harvested, shock frozen in liquid nitrogen and resuspended immediately in 100 ml TMMG buffer (50 m*M* Tris–HCl, 10 m*M* $MgCl_2$, 5 m*M* β-mercaptoethanol, 1.7 m*M* GTP pH 7.5) with 0.4%(*w*/*v*) sodium deoxycholate and two tablets of Complete protease inhibitor (Boehringer). After treatment with DNaseI for 20 min at 277 K, cells were passed through a fluidizer and centrifuged at 100 000*g*. The supernatant was applied onto a GSH Sepharose 4B column equilibrated in TMMG buffer. After extensive washing of the column, cleavage of the tags was carried out with 1200 units thrombin (Serva) overnight. About 120 mg of a complex between PDE δ and ARL2 were eluted in TMMG buffer, concentrated by ultrafiltration and applied onto a Superdex S75 gel-filtration column, from which the complex eluted in the expected volume. Additionally, the identity of both proteins was verified by mass spectrometry and N-terminal sequencing. The complex was concentrated to 29 mg ml^{-1}, dialysed against 50 m*M* Tris–HCl, 10 m*M* $MgCl_2$, 5 m*M* β-mercaptoethanol, 5 m*M* GTP pH 7.5 and stored flash-frozen at 193 K.

For the production of the selenomethionine-labelled complex (Doublie, 1997), *E. coli* B384 cells were grown in LeMaster minimal medium (Hendrickson *et al.*, 1990) with 200 mg l^{-1} ampicillin, 100 mg l^{-1} kanamycin and 50 mg l^{-1} methionine at 291 K and selenomethionine was substituted for methionine at gradual intervals. Protein production was then performed in a 16 l culture with 50 mg l^{-1} selenomethionine. Prior to inoculation, cells were tested for methionine-independent growth and co-expression of both proteins. It was necessary to lower the temperature to 291 K and to reduce the IPTG concentration to 0.2 m*M* to keep the complex soluble. Purification was performed as described for the wild type.

Crystals were grown using the hanging-drop method. All setups were performed at 277 K to minimize GTP hydrolysis. Initial conditions were identified in a PEG screen for 5–10% PEG 6000 at pH 6.0–8.0. Fine-tuning of the condition and extensive streak seeding [in drops consisting of 1 µl protein solution and 1 µl reservoir (9–12% PEG 5000 MME, 0.1 *M* HEPES pH 7.0) and which were pre-equilibrated for 1.5 h over 1 ml reservoir] resulted in larger rod-shaped crystals. The identity of the crystallized material was checked by SDS–PAGE and mass spectrometry of thoroughly washed crystals. The selenomethionine complex crystallized under the same conditions as the wild type. After storage of the crystallization setups for several months at 277 K, a second crystal form was found which recrystallized from the first one.

For the first crystal form, a native data set ('Native-1') to 2.3 Å resolution was collected from one crystal on a MAR CDD detector at the microfocus beamline ID13 (ESRF, Grenoble). The crystal was quickly transferred in two steps into 15% PEG 5000 MME/30% glycerol as cryoprotectant and flash-cooled to 100 K immediately prior to data collection. The data-collection statistics are given in Table 1. For the second crystal form, a native data set to 1.8 Å resolution ('Native-2') was collected at beamline BW6 (DESY, Hamburg) using 15% PEG 5000 MME/15% glycerol/10% xylitol as cryoprotectant. In addition, a SAD data set ('SeMet') for crystal form 2 to 2.6 Å resolution was collected from a selenomethionine-labelled crystal using a MAR CCD detector at beamline ID13 (ESRF, Grenoble), with 20% PEG 5000 MME/10% PEG 400 as cryoprotectant. All diffraction data were processed using *DENZO* and *SCALEPACK* (Otwinowski & Minor, 1997).

Table 1
Data-collection statistics for different crystals of ARL2:PDE δ.

	Native-1 (crystal form 1)	Native-2 (crystal form 2)	SeMet (crystal form 2)
Crystal dimensions (µm)	10 × 60 × 300	400 × 400 × 400	30 × 80 × 100
X-ray source	ID 13 (ESRF)	BW 6 (DESY)	ID 13 (ESRF)
Wavelength (Å)	0.782	1.005	0.964
Detector	MAR CCD	MAR CCD	MAR CCD
Crystal-to-detector distance (mm)	150	200 (low), 108 (high)†	150
Total rotation scan (°)	130	100 (low), 194.6 (high)†	209
Exposure time (s)/oscillation range (°)	2/1	5/1 (low), 12/0.2 (high)†	6/1
Space group	$P2_1$ (No. 4)	$P2_12_12_1$ (No. 19)	$P2_12_12_1$ (No. 19)
Unit-cell parameters			
a (Å)	48.1	44.5	44.8
b (Å)	45.7	65.4	65.7
c (Å)	74.7	104.4	104.0
β (°)	94.0	90.0	90.0
Mosaicity (°)	0.45	0.61	1.20
Resolution range (Å)	19.7–2.3	34.7–1.8	19.8–2.6
Highest resolution shell (Å)	2.35–2.30	1.84–1.80	2.65–2.60
Total No. of reflections	41852	248895	86108
No. of unique reflections	14251	28815	9926
Multiplicity‡	2.9 (3.0)	8.6 (7.9)	8.7 (9.6)
Completeness‡ (%)	97.5 (99.7)	99.5 (98.9)	99.6 (100.0)
R_{sym}‡	0.065 (0.235)	0.042 (0.316)	0.081 (0.391)
$I/\sigma(I)$‡	14.8 (5.8)	38.8 (4.8)	25.1 (7.0)

† Data set 'Native-2' was collected in two sweeps, a low- and a high-resolution sweep (detector edge at 2.7 and 1.7 Å, respectively). ‡ Values in parentheses refer to the highest resolution shell.

3. Results and discussion

Murine ARL2 comprising residues 1–184 fused *via* an amino-terminal linker to GST and human PDE δ comprising residues 1–150 with an additional amino-terminal His tag were co-expressed in *E. coli* B834. Cells with both plasmids produced considerably more PDE δ than cells expressing PDE δ alone and, judging from SDS–PAGE analysis, GST-ARL2 and His-PDE δ were always produced in a 1:1 ratio. This was taken as evidence that both proteins already form a complex in *E. coli* and that GST-ARL2 stabilizes the expression of His-PDE δ. After affinity chromatography *via* the GST-tag of ARL2, thrombin cleavage removed both the amino-terminal His tag of PDE δ and the amino-terminal GST-fusion

of ARL2 in one step. The eluted protein fractions were further purified by gel filtration, which showed a homogenous peak for the stable ARL2:PDE δ complex. As PDE δ shows high binding affinity only to the GTP-bound state of ARL2 (M. Hanzal-Bayer, unpublished work) and inhibits dissociation of GTP once it is bound, we expected the purified complex to contain ARL2 in the GTP-bound form and will refer to it as ARL2-GTP:PDE δ hereafter.

The initially observed clusters of microneedles of crystal form 1 (Fig. 1*a*) grew within 1–5 d and were improved by streak seeding to form rod-shaped crystals with typical dimensions of 30 × 50 × 400 µm (Fig. 1*b*). SDS–PAGE analysis of washed crystals (Fig. 2, lane 2) confirmed the presence of both ARL2 and PDE δ. Mass spectrometry confirmed the identity of the molecules and the expected thrombin cleavage site: the obtained masses (21 006 Da for ARL2 and 17 562 Da for PDE δ) correspond to the expected values for the native sequences with an additional Gly-Ser at each amino terminus as a cloning artefact and the mutation Ser33Leu in ARL2 introduced accidentally by PCR (ARL2 expected MW, 21 008 Da; PDE δ expected MW, 17 564 Da). A Leu is found in this position in the closely related protein ARL3 which interacts with PDE δ in a similar manner (Linari, Hanzal-Bayer *et al.*, 1999). Therefore, we do not consider the Ser33Leu mutation to show an effect on the interaction with PDE δ.

In a first set of experiments on crystals of form 1 at beamline BM30 (ESRF, Grenoble), all the crystals tested exhibited varying degrees of twinning. A 2.7 Å data set was collected from a rod-shaped crystal (~40 × 60 × 300 µm) which showed relatively little twinning (data not shown). However, all attempts to solve the phase problem by molecular replacement using *AMoRe* (Navaza & Saludjian, 1997) with different search models failed with this data set. As smaller crystals showed less twinning, we collected an additional native data set from a crystal of only 10 × 60 × 300 µm in size using the microfocused X-ray beam at beamline ID13 (ESRF, Grenoble). This crystal diffracted to better than 2.3 Å and was indeed devoid of twinning (for statistics, see Table 1). It belongs to the monoclinic space group $P2_1$, with unit-cell parameters a = 48.1, b = 45.7, c = 74.7 Å, β = 94.0°. The Matthews parameter suggests one complex per asymmetric unit, with V_M = 2.1 Å^3 Da^{-1} (solvent content 41%). In this case, molecular replacement using *AMoRe* resulted in clear solutions both for ARL3-GDP (Hillig *et al.*, 2000) and ARF1Δ17-GppNHp (Goldberg, 1998) as search models, producing identical orientations with both models. Electron-density maps calculated with molecular-replacement phases derived from search models where the nucleotide was omitted showed clear density for a nucleotide with three phosphates, thereby confirming that ARL2 did indeed crystallize in the GTP-bound form. Probably owing to an incomplete molecular-replacement search model, the electron density for PDE δ was not yet interpretable.

Meanwhile, a second crystal form with more compact morphology was found in crystallization setups stored for several months at 277 K (Fig. 1*c*). The crystals recrystallize from the rod-shaped crystals of form 1. This process started spontaneously and only in very few of the drops. After a year, however, the transformation had taken place in the majority of the drops and produced large crystals (Fig. 1*d*). SDS–PAGE also confirmed the presence of both proteins in these crystals. One of these crystals was used to collect a native data set to 1.8 Å resolution ('Native-2' in Table 1) on the MPG/GBF wiggler beamline BW6/DORIS (DESY, Hamburg). It showed roughly octahedral morphology with edges of ~400 µm each and was found in a drop which, at the time of data collection, had been stored for 13 months at 277 K. The space group of this crystal form is $P2_12_12_1$, with unit-cell parameters a = 44.5, b = 65.4, c = 104.4 Å. The Matthews parameter is 2.0 Å^3 Da^{-1} (solvent content 37%) for one complex per asymmetric unit. Molecular-replacement attempts with this data set once again revealed density for three phosphates in the nucleotide-binding site, although the search models were still insufficient to produce interpretable density for PDE δ. We therefore initiated the production of the selenomethinine complex (see §2) to solve the phase problem by MAD or SAD phasing. We expected that three methionines in ARL2 and five methionines in

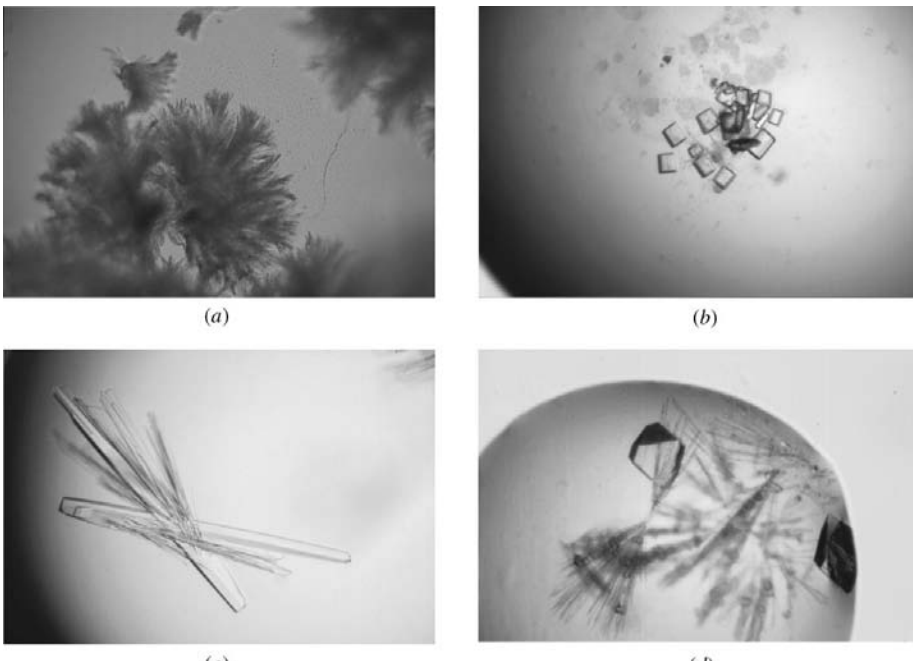

Figure 1
Crystals of ARL2-GTP:PDE δ. (*a*) Clusters of microneedles of crystal form 1 as found with the initial condition. (*b*) Selenomethionine crystals of crystal form 2 (maximum size about 30 × 80 × 100 µm) as used for data set 'SeMet'. (*c*) Rod-shaped crystals optimized by streak seeding as used for data collection. The largest rod has dimensions of ~20 × 40 × 800 µm. (*d*) Large native crystals of form 2 (edges ~400 µm) as used for 'Native-2', found 13 months after setting up of the drop. In the background aged needle bundles of crystal form 1 are still visible.

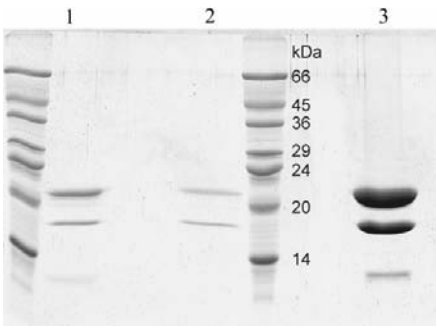

Figure 2
SDS–PAGE analysis of washed and dissolved crystals of crystal form 1. Lane 1, mother liquor taken from crystallization drop; lane 2, washed crystals; lane 3, protein solution as used for crystallization.

PDE δ would be sufficient for successful phasing. Initially, we obtained very thin needles of crystal form 1 which were inappropriate for data collection. However, a crystal of form 2 ($\sim 30 \times 80 \times 100$ µm in size; Fig. 1*c*) allowed collection of a SAD data set to 2.6 Å resolution at the microfocus beamline ID13 (ESRF, Grenoble; data set 'SeMet' in Table 1).

With the data set 'SeMet', we succeeded in improving the quality of the electron-density maps by a combination of molecular replacement and SAD phasing. Preliminary data indicate that the core of PDE δ is appreciably interpretable in both crystal forms. However, some of the loops of PDE δ appear to be well ordered only in form 2, which seems to be a result of better crystal packing. Model building and refinement in both crystal forms is in progress and will be described elsewhere, together with the structure and the detailed phasing procedure.

We would like to thank Heino Prinz for mass-spectrometry measurements, Philippe Carpentier for help with data collection at beamline BM30, Tassos Perrakis for help with data collection at ID13 and repeated access to microfocus beam time, the ESRF for access to synchrotron beam time, Hans Bartunik for fast allocation of beam time at the MPG/GBF wiggler beamline BW6/DORIS (DESY, Hamburg), Gleb Bourenkov for help during data collection at BW6, Balaji Prakash and Caroline Allen for discussions and critical reading of the manuscript and Fred Wittinghofer for ongoing support. LR is supported by an EMBO fellowship (grant ALTF 264-1999). Data collection at ESRF was supported by the European Community Access to Research Infrastructures action of the Improving Human Potential Programme.

References

Amor, J. C., Harrison, D. H., Kahn, R. A. & Ringe, D. (1994). *Nature (London)*, **372**, 704–708.
Antonny, B., Béraud-Dufour, S., Chardin, P. & Chabre, M. (1997). *Biochemistry*, **36**, 4675–4684.
Béraud-Dufour, S., Paris, S., Chabre, M. & Antonny, B. (1999). *J. Biol. Chem.* **274**, 37629–37636.
Chavrier, P. & Goud, B. (1999). *Curr. Opin. Cell Biol.* **11**, 466–475.
Doublie, S. (1997). *Methods Enzymol.* **276**, 523–530.
Goldberg, J. (1998). *Cell*, **95**, 237–248.
Greasley, S. E., Jhoti, H., Teahan, C., Solari, R., Fensome, A., Thomas, G. M. H., Cockcroft, S. & Bax, B. (1995). *Nature Struct. Biol.* **2**, 797–806.
Hendrickson, W. A., Horton, J. R. & LeMaster, D. M. (1990). *EMBO J.* **9**, 1665–1672.
Hillig, R. C., Hanzal-Bayer, M., Linari, M., Becker, J., Wittinghofer, A. & Renault, L. (2000). *Structure Fold. Des.* **8**, 1239–1245.
Kahn, R. A. & Gilman, A. G. (1984). *J. Biol. Chem.* **259**, 6228–6234.
Linari, M., Hanzal-Bayer, M. & Becker, J. (1999). *FEBS Lett.* **458**, 55–59.
Linari, M., Ueffing, M., Manson, F., Wright, A., Meitinger, T. & Becker, J. (1999). *Proc. Natl Acad. Sci. USA*, **96**, 1315–1320.
Menetrey, J., Macia, E., Pasqualato, S., Franco, M. & Cherfils, J. (2000). *Nature Struct. Biol.* **7**, 466–469.
Moss, J. & Vaughan, M. (1998). *J. Biol. Chem.* **273**, 21431–21434.
Navaza, J. & Saludjian, P. (1997). *Methods Enzymol.* **276**, 581–594.
Otwinowski, Z. & Minor, W. (1997). *Methods Enzymol.* **276**, 307–326.
Tamkun, J. W., Kahn, R. A., Kissinger, M., Brizuela, B. J., Rulka, C., Scott, M. P. & Kennison, J. A. (1991). *Proc. Natl Acad. Sci. USA*, **88**, 3120–3124.